Supplementary Material

A portable fiber-optic sensor based on UiO66-lucigenin complex for chloride ion concentration measurement

Runqi Yao[1], Jixing Huang[1], Zelin Gao[1], Hengbiao Zhang[1], Li Yang[2], Dekui Zhang[2], Tuanjie Che[3], YuChao Li[4,5], Honghan Dong[4,5], Xusheng Xia[6], Ning Wang[6], Liyun Ding[1*]

[1] School of Physical Science and Technology, Lanzhou University, Lanzhou, 730000, China.

[2] The Scend School of Clinical Medicine, Lanzhou University, Lanzhou, 730000, China.

[3] Innovation Center of Functional Genomics and Molecular Diagnostics technology of Gansu Province, Lanzhou 730000, China.

[4] MOE Key Laboratory of Soft Soils and Geoenvironmental Engineering, College of Civil Engineering and Architecture, Zhejiang University, Hangzhou 310058, China.

[5] Center for Hypergravity Experimental and Interdisciplinary Research, Zhejiang University, Hangzhou 310058, China.

[6] Material Science and Engineering School, Wuhan University of Technology, Wuhan 430070, China.

KEYWORDS: optical fiber sensor, fluorescence sensing, chloride ion detection, UiO66-lucigenin complex

1 Characterization of UiO-66-NH_2.

Figure S1(a) shows the SEM image of UiO-66-NH_2, revealing that the UiO-66-NH_2 particles have a regular octahedral shape. Additionally, the structure of UiO-66-NH_2 is uniform and exhibits a high degree of crystallinity. The XRD pattern of UiO-66-NH_2 obtained experimentally, alongside the theoretical XRD pattern of UiO-66, is presented in Figure S1(b). The main characteristic reflections of the UiO-66 series are observed at 7.4° and 8.5°. A comparison of the XRD spectra of the laboratory-synthesized UiO-66-NH_2 and the theoretical spectra of UiO-66 shows a high degree of consistency between the two patterns. The chemical composition and bonding configuration of UiO-66-NH_2 were further confirmed by X-ray photoelectron spectroscopy (XPS). The XPS results, shown in Figure S1(c), confirm the presence of the elements Zr, C, N, and O. Figure S1(d) presents the C1s spectrum of UiO-66-NH_2, which reveals four peaks at 284.4 eV, 285.2 eV, 285.9 eV, and 288.6 eV, corresponding to the C-C, C-N, C=C, and O=C-O chemical bonds, respectively. Figure S1(e) displays two peaks at 182.5 eV and 184.9 eV, which can be attributed to the Zr^{4+} $3d_{5/2}$ and $3d_{3/2}$ transitions[1]. The XPS pattern of N 1s shown in Figure S1(f) illustrates two major peaks at 399.3 eV and 400.3 eV, corresponding to the -NH_2 and -NH_3^+ groups, respectively. The peak at 400.3 eV is likely due to proton-amine interactions[2].

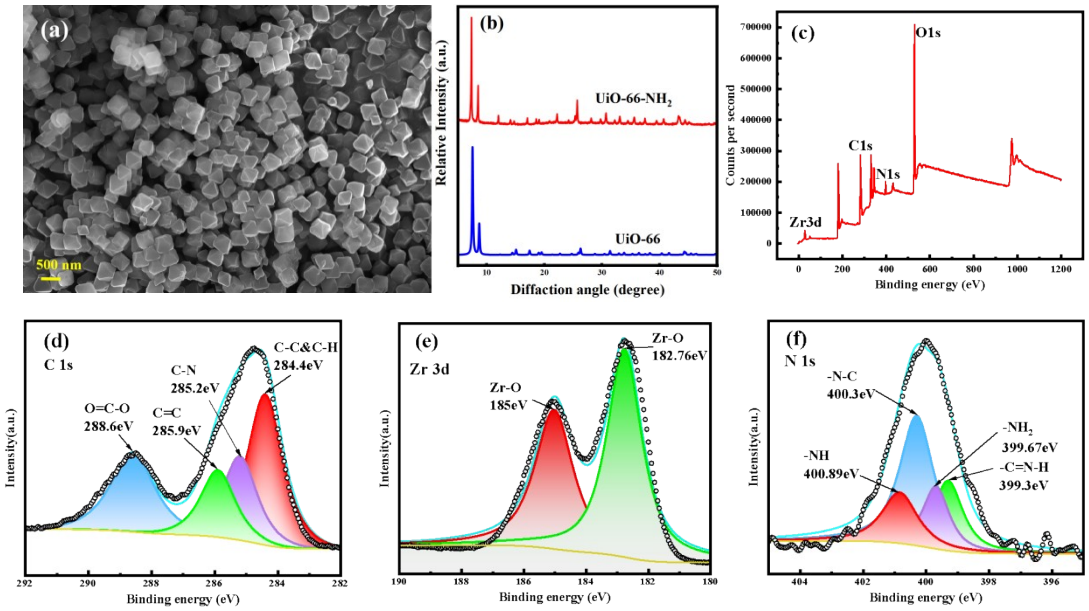

Fig.S1 (a) SEM image of UiO-66-NH_2 (b) XRD patterns of prepared UiO-66-NH_2 and theoretical XRD patterns of UiO-66 (c) XPS of full spectrum (d) XPS spectra of C 1s (e) XPS spectra of Zr 3d (f) XPS patterns of N 1s.

2 Ion interference resistance of the portable chloride ion sensor.

To evaluate the anti-ion interference capability of this portable sensor in complex environments, the following experiments were conducted: as shown in Figure S2(a), the sensing probe was first placed in a 0.3 M NaCl solution, then sequentially transferred into 0.3 M KCl and $CaCl_2$ solutions, and finally into a solution containing 0.1 M NaCl, 0.1 M KCl, and 0.1 M $CaCl_2$ simultaneously. The test results showed minimal variation in signals across these different environments, demonstrating that K^+ and Ca^{2+} do not interfere with Cl^- detection. Meanwhile, as

illustrated in Figure S2(b), the probe was initially placed in a 0.3 M NaCl solution, followed by the sequential introduction of 0.3 M NO_3^-, CO_3^{2-}, SO_4^{2-}, and I^-. The results indicated that these anions also had negligible impact on the detection signal, confirming that the sensor remains unaffected by interference from mixed anions such as NO_3^-, CO_3^{2-}, SO_4^{2-}, and I^-.

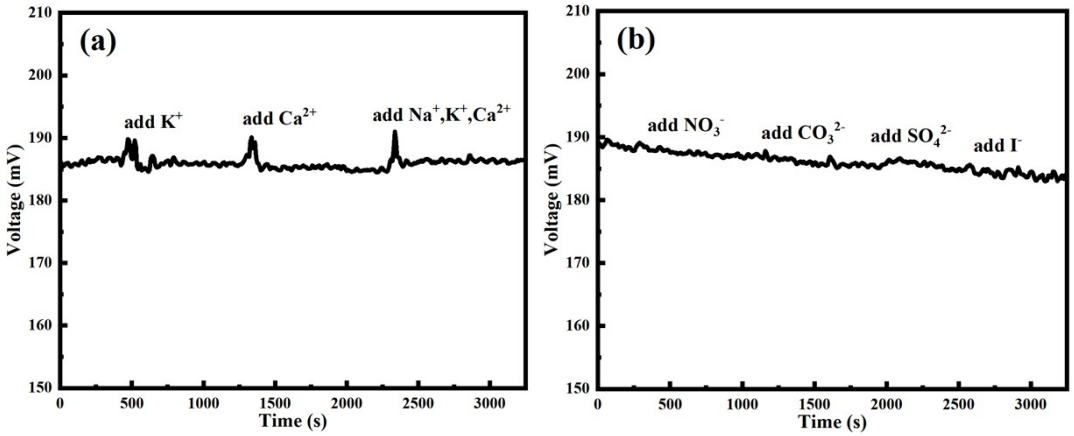

Fig.S2 (a) Cation interference test (b) Anion interference test.

3 Comparison of different chloride ion sensors.

As shown in the table S1, while the coefficients of determination are all close to 1, the chloride ion sensor developed in this study exhibits a significantly broader measurement range compared to other fluorescent chloride ion sensors. In contrast to traditional electrochemical sensors, this optical fiber-based chloride ion sensor demonstrates a notable advantage in resisting ion interference.

Table S1. Comparison of different chloride ion sensors

Detection method	Material	Testing Scope	Coefficient of Determination	References
Fluorescence	UiO66-Lucigenin	0-1M	0.9979	This work
Fluorescence	THPP-Ag+	20-140μM	0.9922	[3]
Electric potential	Flexible Arrayed RuO_2/0.01 wt% GO	10^{-5} -1M	0.972	[4]
Fluorescence	quinine sulfate	0-0.06M	0.99	[5]

4 The repeatability of the batch fabrication of the fiber optic sensing probes.

To investigate the batch-to-batch reproducibility of the fiber optic sensing probes, three batches of fabricated chloride ion probes were tested using 0–1 mol/L chloride ion solutions. The test results are shown in Figure S4. It can be observed that the test results from different batches of fiber optic sensing probes are similar, demonstrating good batch-to-batch reproducibility. The slight deviations in the test results among different probe batches may be attributed to the fact that, although the fabrication method remained consistent, the manufactured probes cannot be guaranteed to be identical.

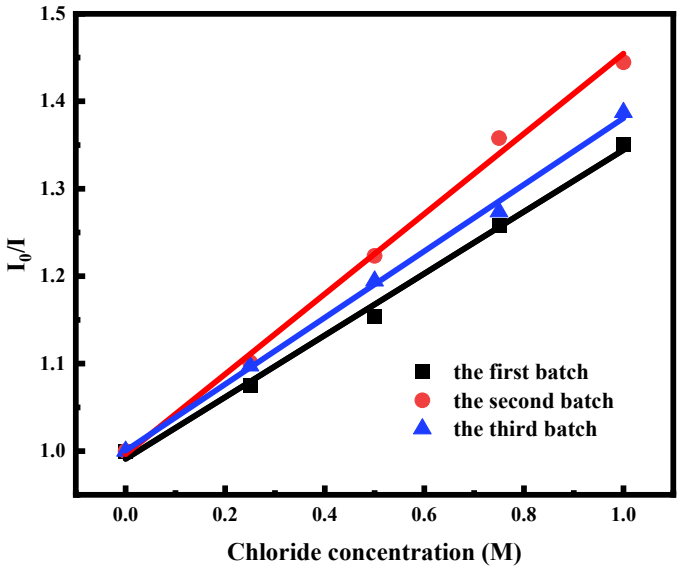

Fig.S3 Fitted calibration curves obtained from tests on different batches of fiber optic sensing probes.

5 Detection of chloride ion concentrations in natural soil.

Using natural soil as the substrate, saturated soil samples containing different chloride ion concentrations were tested with the portable chloride ion sensor. The detection results are shown in Figure S4. The linear regression equation fitted to the data is given by: $I_0/I = 0.2030[Cl^-] + 1.0153$($R^2 = 0.9747$). It can be observed that the fitted curve exhibits good linearity, demonstrating that the portable chloride ion sensor is capable of detecting chloride ion concentrations in natural soil environments.

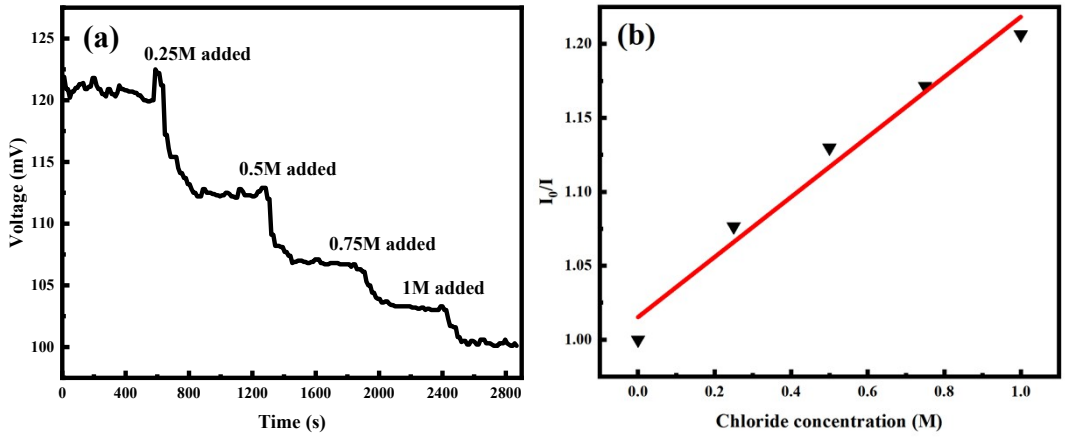

Fig.S4 (a) Time series plot of voltage intensity in natural soil. (b) Fitted fluorescence curves for

different chloride ion concentrations in soil.

6 Detection of Chloride Ions under Different pH Conditions

Solutions with different pH values were prepared using ultrapure water, sulfuric acid, and sodium hydroxide. Using these solutions as the matrix, a series of chloride ion solutions with varying concentrations were prepared and tested with the portable sensor. The detection results are shown in the Figure S5. It can be observed that the sensor performs effectively under all these pH conditions. However, the slope of the fitted curve increases with rising pH.

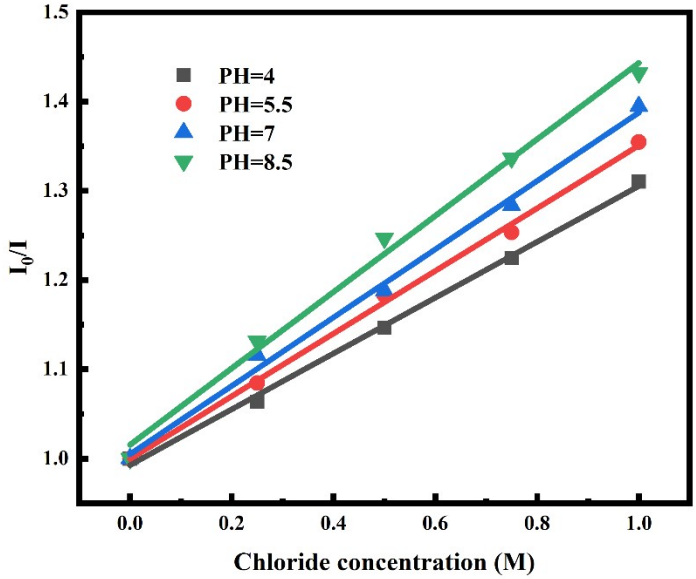

Fig.S5 PH-Dependent Chloride Ion Detection.

6 Detection limit of the portable sensor in soil

Figures 5(f) and 5(g) illustrate the variations in voltage and the corresponding fitting curves under different chloride ion concentrations in sandy soil. The linear regression equation obtained from the data is $I_0/I = 0.1273[Cl^-]+0.9897$($R^2$=0.9866). Furthermore, we calculated the detection limit of the sensor. The detection limit was calculated using the following formula:

$$LOD = 3\sigma/S \quad (1)$$

Here, S is 0.1273, and the standard deviation, determined from multiple measurements, is approximately 0.001592. The limit of detection (LOD) was calculated to be 37.5 mM.

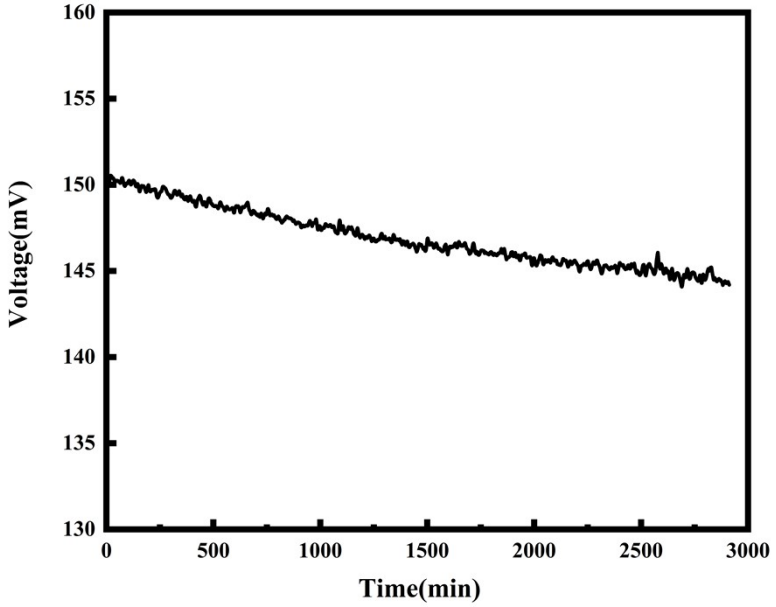

Fig.S6 Stability test in saturated sandy soil containing 0.1 mol/L chloride ions.

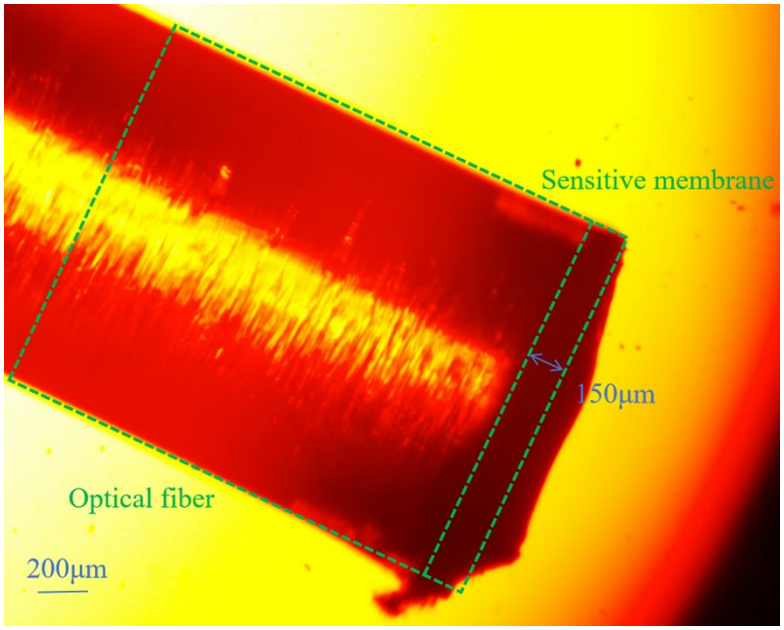

Fig.S7 Thickness of the sensing membrane on the optical fiber probe.

References

[1] Peñas-Garzón M, Sampaio M J, Wang Y L, et al. Solar photocatalytic degradation of parabens using UiO-66-NH2[J]. Separation and Purification Technology, 2022, 286: 120467. https://doi.org/10.1016/j.seppur.2022.120467

[2] Fang X, Wu S, Wu Y, et al. High-efficiency adsorption of norfloxacin using octahedral UIO-66-NH2 nanomaterials: Dynamics, thermodynamics, and mechanisms[J]. Applied Surface Science, 2020, 518: 146226. https://doi.org/10.1016/j.apsusc.2020.146226

[3] Zhang F, Ma C, Jiao Z, et al. A NIR Turn-on Fluorescent Sensor For Detection of Chloride Ions in vitro

and in vivo[J]. Spectrochimica Acta Part A: Molecular and Biomolecular Spectroscopy, 2020, 228: 117729. https://doi.org/10.1016/j.saa.2019.117729

[4] Tseng S C, Wu T Y, Chou J C, et al. Research of sensing characteristic and dynamic measurement of graphene oxides modified flexible arrayed RuO2 chlorine ion sensor[J]. Materials Research Bulletin, 2018, 101: 155-161. https://doi.org/10.1016/j.materresbull.2018.01.015

[5] Lin Z, Ouyang Q, Guo C, et al. Fluorescent Probe-Based Fiber Optic Sensor for Real-Time Monitoring of Chloride Ions in Coastal Concrete Structures[J]. Sensors, 2024, 24(12): 3700. https://doi.org/10.3390/s24123700